Optics Letters

Co-integration of mesoporous GaN distributed Bragg reflectors and light-emitting diodes by transfer printing

Benoit Guilhabert,[1,*] Miles Toon,[1] Saptarsi Ghosh,[2] Dimitars Jevtics,[1] Zhongyi Xia,[1] Menno Kappers,[2] Martin D. Dawson,[1] Rachel A. Oliver,[2] and Michael J. Strain[1]

[1] Institute of Photonics, Department of Physics, University of Strathclyde, Glasgow, G1 1RD, UK
[2] Department of Materials Science and Metallurgy, University of Cambridge, Cambridge CB3 0FS, UK
*benoit.guilhabert@strath.ac.uk

Received 13 November 2025; revised 16 January 2026; accepted 18 January 2026; posted 20 January 2026; published 9 February 2026

Transfer printing is employed to demonstrate the integration of gallium nitride (GaN)-based distributed Bragg reflectors (DBR) with 100 µm lateral dimensions and reflectance of 90% in various formats. Mesoporous GaN DBRs are utilized as basic building blocks to fabricate more complex photonic devices directly on Silicon (Si) and glass receiving substrates. Multi-mode optical resonant cavities centered at 450 nm on Si are thus formed by direct stacking of two mesoporous DBR membranes. Furthermore, active devices are also demonstrated by combining mesoporous DBR with GaN-based light-emitting diodes membranes of similar dimensions, resulting in a Fabry–Perot-mediated emission with its main peak shifted by 14 nm compared to a reference device without DBR. Measured optical bandwidth of 136 MHz (−6 dB) in a small signal modulation scheme is also demonstrated from these devices.

https://doi.org/10.1364/OL.584532

Introduction. New techniques to realize hybrid integration of dissimilar semiconductor materials are maturing to enhance chip capacities by exploiting their best properties. Transfer printing (TP) is one such technique successfully applied in various fields such as telecommunications [1–3], quantum technologies [4–6], flexible displays, and electronics [7,8]. It consists of transferring to a host substrate fully fabricated devices, prepared in membranes format, using selective chemical etching. TP relies on an accurate pick-and-place system to print devices where they are required on a host substrate. Subsequent micro-fabrication techniques can be carried out on the printed devices on the host substrate. Among these demonstrations, blue-emitting gallium nitride (GaN) light-emitting diode (LED) epitaxial structures on silicon (Si) are one of the important optoelectronic components that benefit for on-chip integration. Usually sought after for display applications such as back-lighting or white light generation, they stand on their own as emitters for visible light communication [9], pump light source for chromophores such as light-emitting polymers, colloidal quantum dots [10], nanowire devices [11], and for neuro-photonics [12], to cite a few high-end applications of these devices. More recently, porous GaN distributed Bragg reflectors (DBRs) were also grown and comprise alternating layers of pristine GaN and electrochemically etched Si-doped GaN, resulting in a porous layer [13]. Porous GaN provides not only a larger refractive index contrast to GaN compared to aluminum nitride (AlN) but also a lattice-match characteristics instead of the AlN/GaN ≈2.4% mismatch [14]. Moreover, the extension of the GaN/mesoporous GaN DBR approach grown on Si substrates offers the advantages of cheap scalability with wafers of up to 300 mm-diameter [15] and the ability for epitaxial separation from the substrate for subsequent heterogeneous integration such as TP [16]. In addition, they are vertically conductive [15] and offer a better thermal conductivity compared to dielectric counterparts. They are also suitable for vertical cavity lasers (VCSEL) [17]. The heterogeneous integration by TP of GaN-based mesoporous DBRs is reported here, where DBR membranes are employed as basic building blocks to form more complex devices directly by TP on versatile receiver substrates. Several DBRs are reported to be printed over each other, or one DBR device can act as a local receiver for a different device type e.g., an LED in this case. Previous demonstrations from our group demonstrated consistent successful TP with high placement accuracy for membranes with similar sizes [10,16]. First, fabrication of suspended and tethered membranes with lateral dimensions of 100 $\times$100 µm^2 is presented and their optical characteristics assessed demonstrating that optical reflectance of 90% is preserved after the fabrication and TP processes. TP is also employed to fabricate optical resonators centered at 450 nm directly on a Si receiver chip. The direct stacking of two such DBRs creates multi-mode optical cavities with distinct dips in the reflectance spectrum. Extinction coefficients of about 10% were measured for a free spectral range of 11 nm. Furthermore, the combination of mesoporous GaN DBRs with GaN-based LED is presented. The DBRs and LEDs (hereafter dubbed miniLEDs) were of similar lateral dimensions and the miniLEDs had a designed emission wavelength

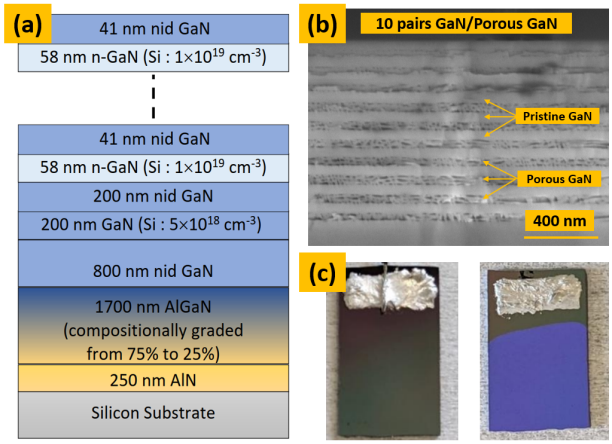

Fig. 1. (a) Schematic structure of the GaN-based DBR showing the buffer and the alternating layer employed. (b) SEM of a representative alternating layer stack of undoped and Si-doped GaN (10 pairs) after ECE showing the presence of pores in the distinct layer of doped GaN. (c) Representative GaN DBR (5 pairs in this specific case) wafer piece (left) before and (right) after ECE showing the change of light reflection behavior.

peaking at 460 nm. The miniLEDs had a spreading layer made of 100 nm-thick Palladium (Pd) that forms with the DBR a cavity as thick as the entire LED epitaxial structure. Changes in electrical luminescence spectra show distinctive peak emitted at approximatively 482 nm with a comparatively similar optical bandwidth to 136 MHz (−6 dB) to reference miniLEDs TP over the same substrate.

Porous GaN distributed Bragg reflectors. The porosification by electrochemical etching (ECE) of Si-doped GaN provides a large refractive index contrast when compared to pure GaN and can be implemented to create photonic devices. Consequently, DBRs based on Si-doped/non-intentionally doped (NID) pairs can be epitaxially grown and provide a suitable platform for III-Nitride devices based on high reflectivity. In this work, mesoporous GaN-based DBRs are grown on <111> Si substrates by metal organic chemical vapor deposition at high temperature. The growth structure comprises an AlN nucleation layer 250 nm-thick followed by a graded layer of $Al_xGa_{1-x}N$ 1700 nm-thick, with a continuously varied molar fraction of Al, x, from 75 to 25%. The growth continues with a NID-GaN layer of 800 nm thickness. Prior to the epitaxy of the DBR-related structure, a 200 nm-thick layer of Si-doped GaN topped with another 200 nm of GaN is deposited. This pair of layers is intended to provide a conductive backplane for the electrochemical etching of the GaN-based DBR. Ten pairs of Si-doped GaN and NID-GaN that will be used to form the DBR are then grown. The number of pairs and their respective thickness are adjusted to achieve the desired reflectance and center wavelength, respectively. Figure 1(a) shows a schematic of the epitaxial structure used to create the GaN-based porous DBR. The entire structure undergoes an ECE step at controlled bias and current flow, until the etch current drops to a baseline level, in 0.25 Molar concentration oxalic acid using a platinum counter electrode. At the optimum bias, the ECE targets only the Si-doped GaN dopant and etches voids (pores) within it. The pores density is controlled to be between 23 and 28%. DBRs with 90% reflectance centered at 450 nm are thus created, corresponding to 10 pairs of GaN/porous GaN with a thickness of 41 and 58 nm. Figure 1(b)

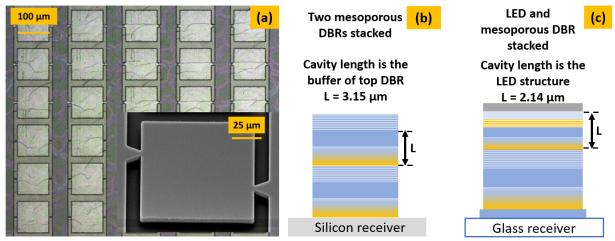

Fig. 2. (a) Micrograph of an array of suspended mesoporous GaN-based DBR ready for TP. Inset, an SEM of a suspended representative mesoporous GaN DBR membrane. Schematics of the structures made by TP, (b) 2 mesoporous DBRs, and (c) one LED and one mesoporous DBR stacked.

is a SEM cross-section imaging of representative alternating layers of GaN and porous GaN showing the formed pores by ECE at 5 V. The ECE propagates through the undoped GaN, through nano-scale channels etched at dislocation cores [18], without affecting it significantly and etches voids only within the Si-doped GaN. Figure 1(c) shows pieces of DBR epitaxy before (left) and after ECE (right), showing a distinctive reflection of the blue region of the visible spectrum when illuminated by a white light source. Further details on the porous microstructure and associated reflectance against the ECE voltage can be found in [19].

Optical cavities made from porous GaN DBR membranes. The GaN-based mesoporous DBRs require first to be fabricated into membranes. This is achieved by securing them to the growth wafer using tethering protocols by first a chlorine-based plasma etching down to the Si substrate, and then a chemical anisotropic etching step with a potassium hydroxide/deionized water solution (concentration of 0.665 g/mL) heated up at 85°C to selectively etch the <110> crystal plane of the Si substrate only [10,20]. Figure 2(a) shows a micrograph of an array of mesoporous GaN DBR membranes, suspended and tethered on the growth Si wafer. The dark vertical rails between each column of membranes are the epitaxial layers still in contact with the substrate, while each membrane shows a clearer coloration due to an air gap between the AlN bottom layer and the Si substrate. Inset of Fig. 2(a) shows a scanning electron microscopy image of a single representative 100 µm × 100 µm membrane as suspended and tethered on the Si growth substrate.

These membranes had 10 pairs of repeated NID-GaN/mesoporous GaN for a reflectance of 90% around 450 nm. A TP method is employed to displace these membranes deterministically to another Si host substrate individually using a system as reported in [16]. Several DBR membranes are employed as elementary building blocks that can be assembled in different configurations, e.g., by printing a secondary DBR membrane directly onto a preprinted one. Figure 2(b) shows a schematic of the structure thus formed. The combinations of these two DBR membranes form optical resonant cavities where the cavity length L is the thickness of the buffer layers of the top membrane, 3.15 µm-thick. The cavity is therefore made of multiple alloys with different thicknesses and refractive indices. Such a cavity length is largely multi-modal in the blue region of the visible optical spectra of light around 450 nm. Reflectance spectra were measured prior to processing, as a single membrane and in the cavity configuration, the latter two TP on Si, using a modified microscope with a white LED as illumination, a 50× objective and with a 0.1 nm-resolution Avantes fibre-coupled spectrome-

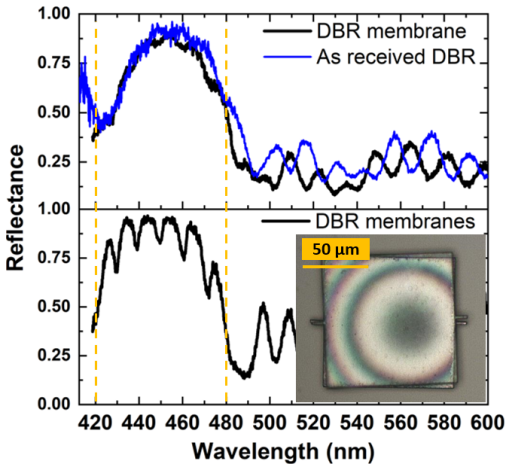

Fig. 3. Top panel is a measured reflectance of a representative mesoporous GaN-based DBR. Bottom panel is the reflectance measured of a stack of 2 mesoporous GaN-based DBRs showing resonances from the buffer cavity thus formed and, inset, two GaN-based DBR membranes TP on top of each other on a Si receiver.

ter and calibrated against a reference aluminum-coated metallic mirror. The top panel of Fig. 3 compares the typical reflectance spectra of a single DBR chiplet as TP onto a Si receiver and of the as-received structure. 90% reflective power was measured around 450 nm as per design against 95% for the as-received representative reflectance spectra, indicating that the membrane process does not deteriorate the GaN-based DBR performances. The bottom panel of Fig. 3 is the reflectance spectra of a representative GaN-based mesoporous DBR cavity. Multiple dips in the reflectance spectra are clearly seen. They have extinction coefficients of about 10% located at wavelengths of 429.6, 438.5, 449.7, 460.6, and 471.7 nm (free spectral range 11 nm), and individual peaks bandwidth at full width at half maximum of 3 nm. The inset shows a micrograph of stacked GaN mesoporous DBR membranes. The ring patterns is the optical interference fringes of the illumination white light indicating a varying air gap between the DBRs stack and the substrate, i.e., membrane with a slight curvature. This can also explain the discrepancies in the reflectance noticeable in Fig. 3 (top panel), although native variation of reflectance spectra across the as-received DBR wafer is also expected. Fully flat membranes suspended from the growth wafer can be obtained by careful optimization of the growth condition where examples and strategies can be found elsewhere [20]. With the addition of a suitable spacer and a flipped TP method as demonstrated in [16], single mode cavity would be achievable, expanding the technique to VCSEL.

Porous GaN DBR chiplets in tandem with blue-emitting light-emitting diodes. The mesoporous GaN DBRs were combined with GaN-based 460 nm-emitting miniLEDs with Palladium (Pd) as spreading p-doped GaN contact as depicted in the schematic in Fig. 2(c). The cavity thus formed has a length L of 2.14 µm corresponding to the thickness of the miniLED. The micro-fabrication of these miniLED devices was reported in [10]. The receiver substrate here is a glass cover slip prepared with SU8 plinths with a thickness of 2 µm for accurate positioning of the DBRs and miniLEDs for subsequent steps. For reference, miniLEDs were placed directly onto these plinths. In the case of the mesoporous DBR/miniLED tandem devices, the GaN mesoporous DBRs were first TP over the plinths, and

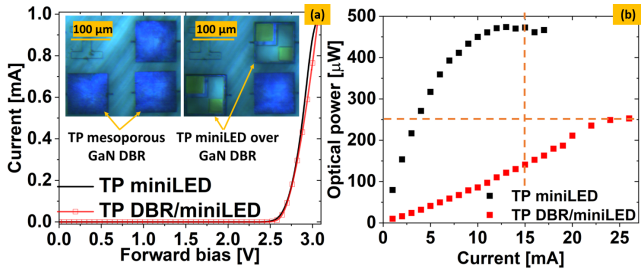

Fig. 4. (a) Current against forward bias voltage and (b) optical power against injected current for representative TP miniLED and DBR/miniLED tandem device. Inset of (a), micrographs of (left) the DBR/miniLED TP process with the mesoporous DBRs TP over the SU8 plinth and (right) the miniLEDs TP over the mesoporous DBRs.

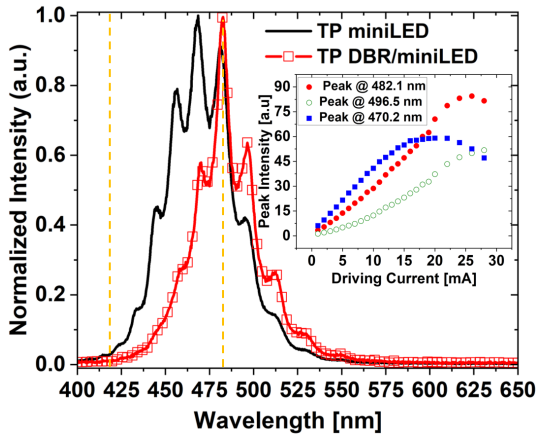

Fig. 5. Emission spectra as measured through the receiving substrate (glass) for a TP miniLED and a mesoporous DBR/miniLED tandem device at 20 mA injected current. Inset: evolution of the main peaks against inject current emitted by the mesoporous DBR/miniLED tandem.

the miniLEDs were subsequently TP over the DBR as shown in the inset of Fig. 4. The devices were then insulated using ParyleneC deposited by evaporation, patterned to create vias onto the devices' contact areas, and metal tracks made of Titanium and Gold (50 and 200 nm, respectively) were patterned by liftoff to allow electrical addressing of the devices. Figure 4(a) shows the current against forward bias voltage traces of the devices with a maximum current compliance of 1 mA showing a nominal voltage of 3 V at compliance current. The emitted optical power and the emission spectra of the reference miniLED and the mesoporous DBR/miniLED tandem devices were then assessed. The collection was done through the glass substrate using imaging optics comprising two achromatic doublets of focals 100 and 50 mm. The maximum projected optical power was measured at 250 µW at 25 mA injected current (470 µW at 15 mA for the reference miniLED), Fig. 4(b), with a roll-over at larger injected current attributed to better thermal management provided by the mesoporous DBR. Figure 5 shows the respective electro-luminescence of both devices with an injected current of 20 mA. The reference TP miniLED shows distinctive peaks emitted at 456, 468, and 482 nm. Instead of the continuous emission, the peaked emission is directly due to the absence of substrate: an intrinsic cavity is formed by the high refractive index contrast between the GaN buffer (2.4) and the under-

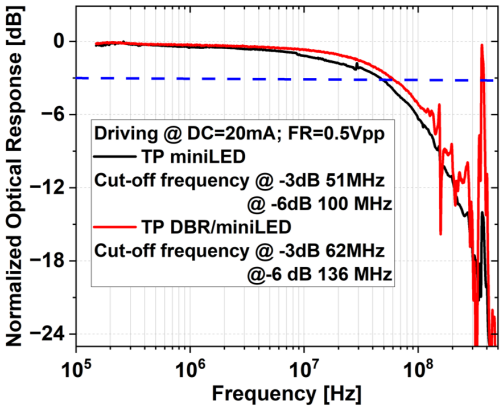

Fig. 6. Frequency response of the TP miniLED and mesoporous DBR/miniLED tandem devices under the small signal modulation addressing scheme.

lying medium: glass/SU8 (1.5) or air. Owing to this contrast, reflection coefficients of approximatively 5 and 12.8% are expected, respectively. A micro-cavity is thus formed in combination with the spreading metal (Pd, reflection of approximatively 60% at 450 nm) and acts on the miniLED spectral emission by Fabry–Perot (FP) effect [21]. In contrast, the mesoporous DBR/miniLED tandem device shows a prominent emission of the peak at 482.1 nm. The effect of the mesoporous DBR is to further select modes of emission from the miniLED by creating a micro-cavity with a higher quality factor. A resonant cavity device is not claimed here as the miniLED epitaxy structure was not optimized to guarantee mode distribution overlap with the quantum well. It is rather shown that the emission modes directly falling within the high reflectivity band of the mesoporous DBR are trapped within the micro-cavity, which allows the modes with preferentially lower reflectance to escape the device. The dashed lines in the figure provide a guide to the eye of the mesoporous DBR reflectance bandwidth (see also Fig. 3). Inset of Fig. 5 shows the evolution of the mesoporous DBR/miniLED emitted peaks against injected current showing that the major emission at 482.1 nm becomes dominant at injected current of about 16 mA. Finally, a small signal frequency response characterization was carried out on both device configurations to extract the optical bandwidth of the devices. The representative mesoporous DBR/miniLED was driven at a direct current injection of 20 mA and a 0.5 V*pp* amplitude sinusoidal signal was added with a frequency varied from 0.15 to 500 MHz. The electrical (and optical) bandwidth at −3 dB (−6 dB) of the mesoporous DBR/miniLED was 62 MHz (136 MHz), similar to 51 MHz (100 MHz) of the miniLED without DBR as shown in Fig. 6. The modulation bandwidths are of the same order of magnitude and no increase in the spontaneous emission rate by Purcell effect is claimed here; the difference is rather attributed to a variation device-to-device from the epitaxial structure or form the microfabrication process.

Conclusions. The capabilities of heterogeneous integration using TP were exploited here to show, in particular, that optoelectronic devices can be micro-fabricated by TP from a set of basic building blocks. Optical resonant cavities were demonstrated by assembling GaN-based mesoporous DBRs directly onto a Si receiver chip. The single chiplet elements were fabricated separately and TP was employed to stack chiplets on top of each other. Optically characterization shows that individual DBR chiplets retained their 90% reflectance property centered at 450 nm. The cavities formed by TP showed distinct multiple resonance peaks within the bandwidth of single DBR reflectance spectra with a free spectral range of 11 nm. Furthermore, GaN miniLEDs TP over mesoporous DBRs were also characterized showing distinct electro-luminescence with centered emission at 482 nm, 14 nm shifted compared to a reference miniLED, 250 µW power and bandwidth at 136 MHz (−6 dB) in a small signal modulation addressing scheme.

Funding. UKRI Engineering and Physical Sciences Research Council HeteroPrint project (EP/R03480X/1); Royal Academy of Engineering (Research Chairs and Senior Research Fellowships); Department for Science, Innovation and Technology (DSIT) Chairs in Emerging Technologies Scheme.

Acknowledgment. The authors acknowledge Porotech, Impington, U.K., for performing the ECE of the GaN samples before TP. Support from the UKRI Engineering and Physical Sciences Research Council, the Royal Academy of Engineering, and the Chairs in Emerging Technologies Scheme, sponsored by DSIT, are acknowledged for financial support.

Disclosures. The authors declare no conflicts of interest.

Data availability. Data underlying the results presented in this paper are available in Ref. [22].

REFERENCES

1. G.-H. Duan, C. Jany, A. L. Liepvre, *et al.*, IEEE J. Sel. Top. Quantum Electron. **20**, 6100213 (2014).
2. G. Muliuk, N. Ye, J. Zhang, *et al.*, in European Conference on Optical Communication (ECOC) (IEEE, 2017), p. 1.
3. J. Zhang, G. Muliuk, J. Juvert, *et al.*, APL Photonics **4**, 110803 (2019).
4. J.-H. Kim, S. Aghaeimeibodi, J. Carolan, *et al.*, Optica **7**, 291 (2020).
5. A. W. Elshaari, A. Skalli, S. Gyger, *et al.*, Adv. Quantum Technol. **4**, 2100032 (2021).
6. J. H. Kim, S. Aghaeimeibodi, C. J. K. Richardson, *et al.*, Nano Lett. **17**, 7394 (2017).
7. S.-I. Park, Y. Xiong, R.-H. Kim, *et al.*, Science **325**, 977 (2009).
8. C. A. Bower, M. A. Meitl, B. Raymond, *et al.*, Photon. Res. **5**, A23 (2017).
9. P. Tian, J. J. D. McKendry, Z. Gong, *et al.*, J. Appl. Phys. **115**, 033112 (2014).
10. K. Rae, P. P. Manousiadis, M. S. Islim, *et al.*, Opt. Express **26**, 31474 (2018).
11. Z. Xia, D. Jevtics, B. J. E. Guilhabert, *et al.*, ACS Nano **19**, 15813 (2025).
12. A. Boudet, R. Scharf, M. D. Dawson, *et al.*, Frontiers in Optics 2016, OSA Technical Digest (Optica Publishing Group, 2016), paper FTh4D.5.
13. C. Zhang, S. H. Park, D. Chen, *et al.*, ACS Photonics **2**, 980 (2015).
14. J.-F. Carlin, C. Zellweger, J. Dorsaz, *et al.*, Phys. Status Solidi B **242**, 2326 (2005).
15. T. Zhu, Y. Liu, T. Ding, *et al.*, Sci. Rep. **7**, 45344 (2017).
16. B. Guilhabert, S. P. Bommer, N. K. Wessling, *et al.*, IEEE J. Sel. Top. Quantum Electron. **29**, 7900111 (2023).
17. S.-M. Lee, S.-H. Gong, J.-H. Kang, *et al.*, Opt. Express **23**, 11023 (2015).
18. F. C.-P. Massabuau, P. H. Griffin, H. P. Springbett, *et al.*, APL Mater. **8**, 031115 (2020).
19. S. Ghosh, M. Sarkar, M. Frentrup, *et al.*, J. Appl. Phys. **136**, 043105 (2024).
20. B. Spiridon, M. Toon, A. Hinz, *et al.*, Opt. Mater. Express **11**, 1643 (2021).
21. C. Hums, T. Finger, T. Hempel, *et al.*, J. Appl. Phys. **101**, 033113 (2007).
22. B. Guilhabert, M. Toon, S. Ghosh, *et al.*, ""Co-integration of mesoporous GaN distributed Bragg reflectors and light-emitting diodes by transfer printing data"," Univ. of Strathclyde (2026), https://doi.org/10.15129/6b76ccf4-0369-4849-9752-81ff4f075c95.